



**Acoustics'08
Paris**
June 29-July 4, 2008

www.acoustics08-paris.org

Broadband scattering from spherical shells in a waveguide: modeling and classification

John Fawcett

DRDC Atlantic, PO Box 1012, Dartmouth, NS, Canada B2Y 3Z7
john.fawcett@drdc-rddc.gc.ca

In this paper, a multipath expansion method is used to model the scattering from a sphere in a Pekeris waveguide. It is shown to be in very good agreement with an exact wavenumber integral representation except when the sphere is very close to the upper pressure release surface. The multipath model is used to model the scattering from a large set of spherical shells of different radii, relative thicknesses, and different materials. The spheres are grouped into six classes and the classification of the spheres from their echos or backscattered spectra is considered, first for the spheres in free space and then for the spheres in the waveguide.

1 Introduction

This paper consists of two basic parts. First, a numerical model is presented for a simple Pekeris waveguide which models scattering from a spherical shell utilizing a multipath expansion for both the incident and scattered fields. This is compared to an exact wavenumber integral approach which can include all orders of target/boundary scattering [1,2](i.e. not just the single scattering approach [3]). It has been shown (e.g., [1-3]) that surrounding boundaries can significantly change the strength and the character of an object's echo. Various authors [4-7] have considered the classification of targets in free space and within a waveguide or near interfaces. In [7] the free-space spectra for a large number of spheres and infinite cylinders of varying radii, thickness, and materials were generated and it was shown that thin and thick-shelled objects could be accurately discriminated by simply using the absolute spectral values as an input feature vector. However, it is not clear whether this approach is still useful when the echo being classified is from an object within a waveguide. In this paper, we will generate many spectra from a large set of spheres which will be subdivided into 6 basic classes. The classification problem for these spheres in free space and in a waveguide will be considered. The spheres will be classified on the basis of their backscattered spectra or time series.

2 Modeling

The scattering of sound from a spherical shell can be analytically described by a sum of spherical harmonics. The coefficients of the harmonics are determined by solving a system of equations which depend parametrically upon the layers and materials of the sphere. The multipath or image expansion method of modelling propagation in a simple waveguide is well known [8]. We will consider the set of $R+1$ rays which connect the specified source position to the centre of the sphere. The appropriate plane wave reflection coefficient is used for each reflection off the seabed and a coefficient of -1 applied for each reflection off the top surface. For each combination of the incoming and outgoing rays, the angular difference at the sphere is computed, and the complex amplitude of the two-way propagation term for the 2 rays is multiplied by the far-field scattering coefficient, $S(\Delta\phi)$, for the particular angular difference. This computation is done for each frequency of interest by using the computed frequency-dependent, free-space scattering coefficients for the sphere. This is similar to the method of [9] for modal conversion at a scatterer. The final expression for the scattered field for a coincident source/receiver is given by

$$p^{sc}(r, z; k) = \sum_{n,m=0}^R \varepsilon_{nm} V(n) V(m) \frac{\exp(i k (D_n + D_m))}{D_n D_m} \times S(\phi_n - \phi_m) \quad (1)$$

where D_n is the source/sphere distance for the n th ray, ϕ_n and ϕ_m are the angles that the incoming and outgoing rays make with respect to the sphere, $V(n)$ is the product of the various reflection coefficients (one for the direct path), S is the sphere's scattering function, and $\varepsilon_{pq}=2$, except for $p=q$ in which case $\varepsilon_{pq}=1$. We take the sphere to be stationary; however, the method can be straightforwardly modified to allow for doppler shifts along the various multipaths. For the following examples in this paper we consider a Pekeris waveguide, 20m in depth. The source and receiver are colocated 0.5m off the seabed. The compressional sound speed of the seabed is 1700m/s with an attenuation of 0.25 dB/ λ . The density is taken to be 1.5g/cm³. The water has a sound speed of 1500m/s and a density of unity. The sphere is at a horizontal range of 200m. We allow 6 bottom reflections in our expansion computations. The other computational method is based upon the wavenumber integral expressions given in [1] and [2]. In particular, our implementation is described in [10] and includes the sphere/boundaries rescattering terms.

In Fig.1 we show the computed spectra, (for the waveguide and geometry described above, multipath method) as a function of sphere depth and frequency for one of the spheres which will be included in our classification study: steel-shelled, evacuated interior, 0.253m radius and a relative thickness of 2.5%. As can be seen, the waveguide modifies the spectra of the echo with an interference pattern. However, some of the spectral features of the free space spectra, such as strong resonances and nulls, persist in an average sense. Figure 2 shows a comparison between the benchmark wavenumber integral results (blue) and the multipath method (black-dashed) results as a function of the sphere's depth for 4 different frequencies. The agreement is very good at the 4 frequencies. The lower panel in Fig.2 shows a comparison of the 2 methods as a function of frequency for 5 different depths. The first depth of 0.26m corresponds to the top surface of the sphere almost touching the water/air interface and there is noticeable disagreement in the region of the strong resonances. Much of this disagreement is due to the rescattering terms which are important for this case. However, the rescattering effects become small by the time the sphere is at a depth of approximately 0.5m. As can be seen, the agreement between the 2 methods is very good for the other depths. For the depth of 19.74m, the bottom surface of the sphere is almost touching the seabed - however, in this case, the differences between the exact and multipath computations are small.

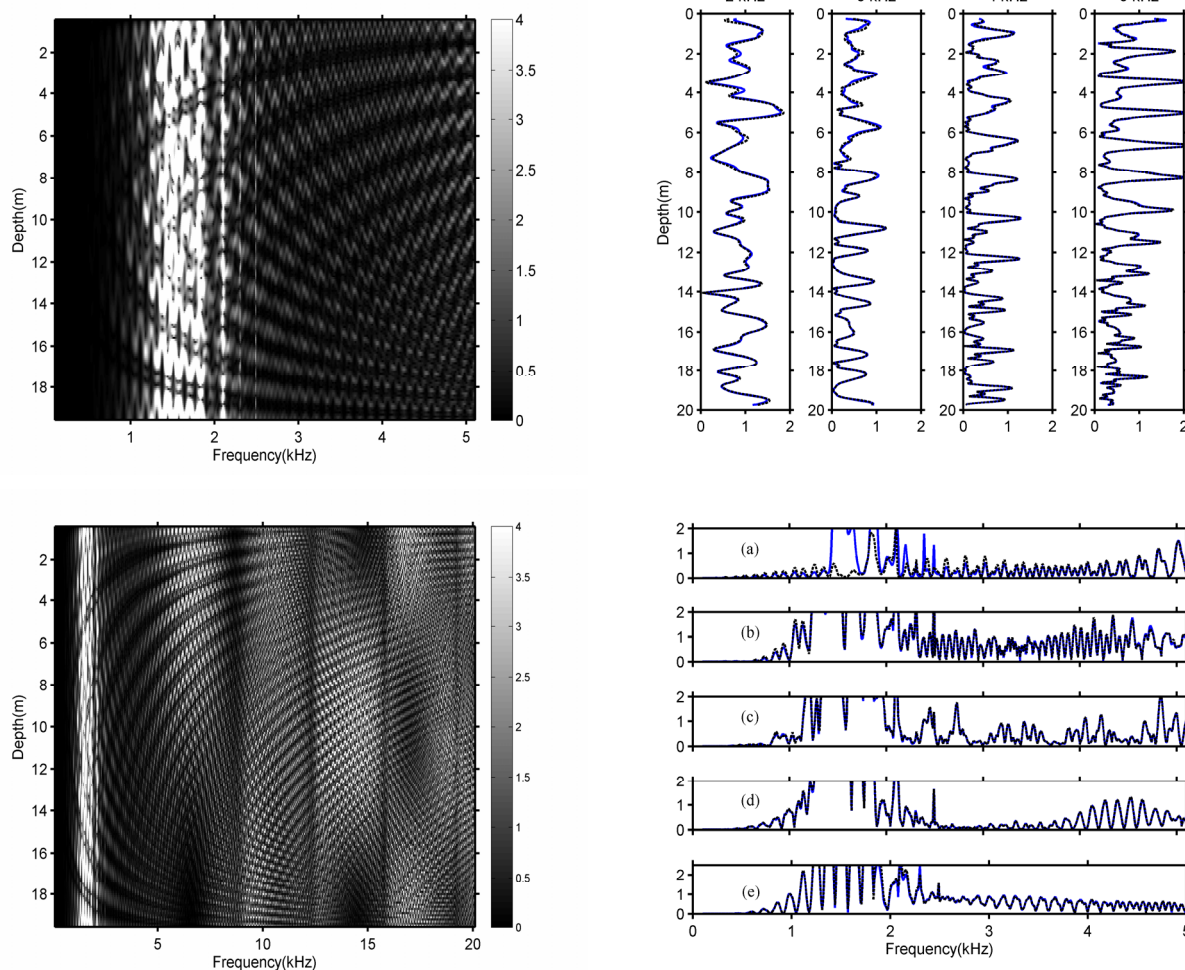


Figure 1 (top) The backscattered spectra as function of frequency [100 5100] Hz and depth for the steel-shelled sphere (bottom). The backscattered spectra for the frequency interval [100 20100] Hz. The amplitudes have been multiplied by a factor of 4×10^4 .

3 Classification

The scattering coefficients and the backscattered spectra [100 20100] Hz. are computed for a large set of spheres in free space at a 10-Hz spacing. This corresponds to a time window of 200 msec. We consider 3 basic material types: (a) steel-shell, evacuated (b) aluminum shell, evacuated and (c) steel-shelled with an interior fill of resin [11]. For each of these cases, there are 31 sphere radii varying from 0.2 to 0.4m and for each of these radii, the relative thickness was varied in a logarithmic fashion from 1% to 99.5% in 21 steps. This results in a total of 1953 spheres. Each of the 3 material classes is subdivided into 2 classes, thin-shelled (relative shell thickness < 10%) and thick ($\geq 10\%$). Thus, we have Class 1, [thin-shelled, steel, evacuated interior], Class 2, [thick-shelled steel, evacuated interior], Class 3 [thin-shelled, aluminum, evacuated interior], etc. We first consider the free-space classification of these spheres, where a training set of just the odd indices (for radii and relative thickness) are used in the training set and the

Figure 2 (top) A comparison of the spectra as a function of depth: the exact wavenumber integral results are in blue and the multipath is black and dashed (bottom) a comparison of the exact (blue) and multipath (black-dashed) methods as a function of frequency for depths of 0.26m, 1.0m, 10m, 19m, 19.74m

remainder are used in the testing set. In this case, the size of the training set is only about 25% of that of the testing set. Here, and in the later examples, the “training” set is, in fact, a library of existing signatures. For the following results we consider a linear Chirp incident pulse, [2 18]kHz over 10 msec. In the top panel of Fig.3 we show in (a) the computed theoretical spectra, weighted by the source spectrum, for a steel-shelled sphere (the same as that used for Fig.1) (evacuated) and (b) the resulting time series (for a source/receiver 10m away). As can be seen from these figures, the low frequency resonances of the steel-shelled sphere are still present due to their very large amplitude, but this portion of the spectrum is, on average, quite close in amplitude to that of the higher frequencies. In practice, if one considers the FFT spectra of a shorter time window of the time series, the resulting spectra have reduced sharp resonances. In the other 2 plots of this panel, we show the spectrum and corresponding time series for the same steel-shelled sphere but with the interior fill. Both the spectrum and the time series are quite different from the evacuated interior case. However, there may be another steel or

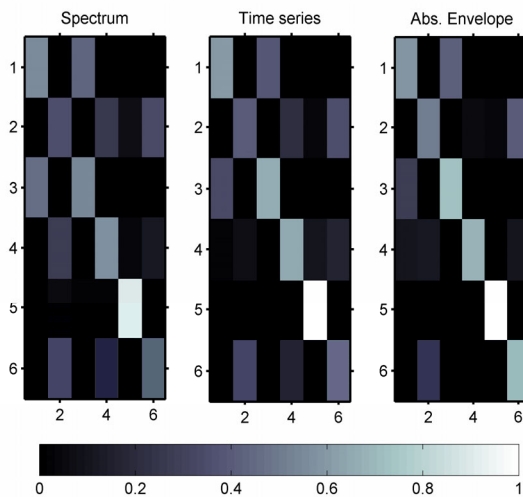
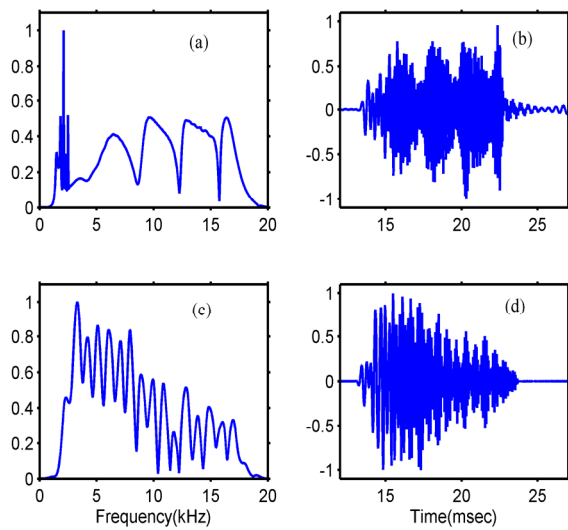


Figure 3 Top: (a) The backscattered spectrum, with source spectrum weighting, for steel-shelled sphere (evacuated interior) (b) corresponding echo time series (c) the backscattered spectrum for steel-shelled sphere with interior fill (d) the corresponding echo time series. Bottom: The resulting Confusion matrices for the 3 different “matching” methods described in the text.

aluminum-shelled sphere (e.g., thicker shell) which more closely matches this particular sphere. In the lower portion of Fig. 3, we show the Confusion matrices which result when (a) the spheres are classified by matching the absolute values (unity L_2 norm) of the spectra from the testing and training sets (the one which gives lowest sum of differences is used for the classification) (b) using the maximum absolute value of the envelope of the cross-correlation between the time series of the test sphere and the training set spheres and (c) matching the absolute values of the envelopes. As can be seen, the best results are obtained by using the absolute values of the envelopes. There is some confusion in the classification results for all 3 approaches but this is expected. For example, some of the thin-shelled steel spheres may be confused with the thin-shelled aluminum spheres (Classes 1 and 3) and vice versa. The thick-shelled, interior-filled steel sphere (Class 6) may be confused with the thick-shelled evacuated steel sphere

(Class 2). However, in general, the thin-shelled spheres are well discriminated from the thick-shelled spheres. The thin-shelled, resin-filled sphere is well classified. We now consider the same set of spheres used for testing in free space and consider them in the waveguide at 2m below the upper surface - the spectra and the time series are computed for this case using the multipath expansion method. There are several different strategies which can be used for echo classification. One can take an entire section of the echo, including the various multipath arrivals, and attempt to match the spectra or time series of the free space results with the observed spectra or time series. We have found that this approach sometimes yields quite good Confusion matrices (some sphere depths or ranges) but often not. One can also extract the first portion of the recorded echo and match this with the free space echos. When the multipath arrivals are sufficiently separated in time, the first portion of the echo will correspond to a direct incident /scattered path and this approach will work well. However, in many situations of interest, the direct and surface reflected paths will have very similar travel times. The other approach is to generate the echos (or spectra) for the training set at different hypothesized depths and to use these for the matching. In Fig.4, top panel, we show the spectra and pulses for the same 2 spheres as Fig.3, but now for the spheres in the waveguide at 2m depth. As can be seen, these spectra and timeseries are significantly different than those of Fig.3. In the bottom portion of Fig.4 we show in (a) the Confusion matrix resulting when we match the spectra (absolute values) of the testing set with the free-space training set. In this case, although the spectra are originally generated at a 10-Hz spacing to construct the timeseries, we take a FFT of 500-point sections of the first portion of the signals (both training and testing sets) to obtain a 250-point spectrum which we use for matching (b) the Confusion matrix resulting when we match the spectra, where the training set spectra are those for a sphere at 1.9m depth (c) the Confusion matrix resulting when we match timeseries (maximum value of the envelope of the cross-correlation) of the testing set (560-point section of the leading part of the echo) with the free space training set and (d) the Confusion matrix resulting when we match the testing set timeseries with the training set generated for 1.9m depth. As can be seen, the freespace spectral matching (a) yielded poor results, whereas matching with replicas from a depth 0.1m in error (b) yielded good results (comparable to the free space results of Fig.3). In the case of the time series matching, using the free space signatures for matching yielded some useful classifications, but using the signatures for the 1.9m depth yielded much better classification results.

4 Summary

We have shown in this paper that the scattering by a spherical elastic shell can be accurately modelled within a simple Pekeris waveguide. Two types of models were considered, an exact wavenumber integral approach and a multipath expansion approach. It was found that the rescattering terms of the sphere with the surrounding boundaries could be significant for the sphere very close to a boundary (in our example, the upper surface). In general,

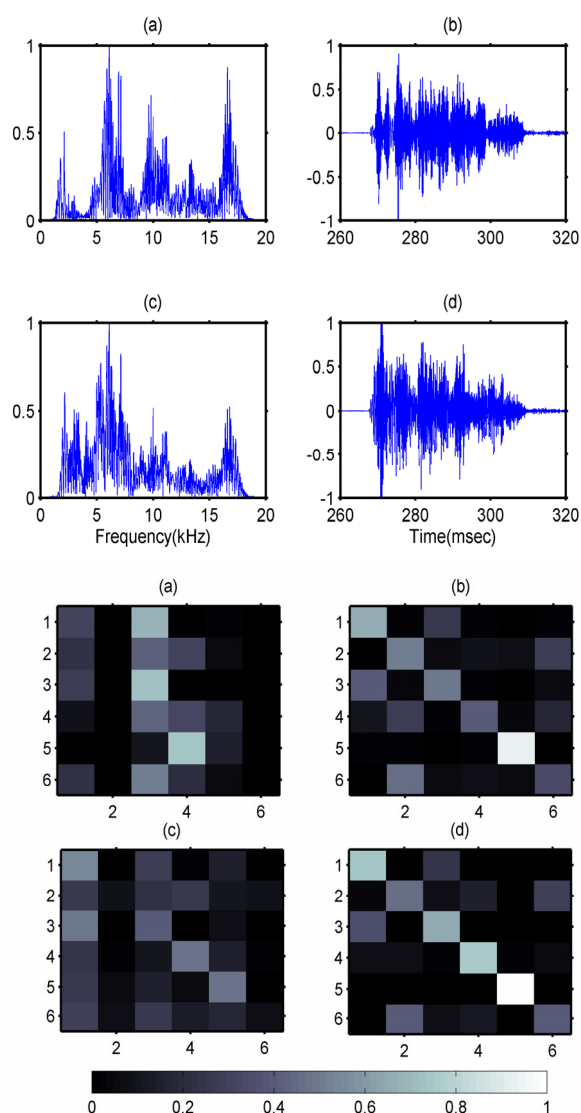


Figure 4 Top: (a) The backscattered spectrum (waveguide, 2m depth) for steel-shelled sphere (evacuated interior) (b) the corresponding echo time series (c) the backscattered spectrum for the sphere with interior fill (d) the corresponding echo time series. Bottom: The Confusion matrices resulting from matching free space spectra and time series (a) and (c) and from matching with spectra and time series (b) and (d) using training set for 1.9m depth. Only the first portion of the echo timeseries is used for the classification.

the approximate, but computationally faster multipath expansion approach yielded accurate spectral and pulse computations. This model was then used to generate spectra and pulses for the scattering from a large set of spheres in a waveguide. The classification study is somewhat simplistic as we considered an omnidirectional source and receiver and ignored any reverberation effects which would be present in a real scenario. However, the study illustrated the complications which the waveguide introduces to the signal classification problem. Although, it is sometimes possible to classify an object in a waveguide using the free space signatures, the classification performance is improved by using signatures for a depth sufficiently close to the true depth (and range) of the sphere. We are currently investigating methods for rapidly generating the training set

for different sphere depths, ranges, and Doppler shifts. In practice, of course, there are many underwater objects of interest which are not spheres. However, using the methods of this paper, large sets of spectra and echos from a wide variety of spheres can be efficiently generated for the spheres in free space and within a waveguide. Thus, this class of object can be very useful for investigating signal processing and classification issues. There are many interesting signal processing issues to explore, optimal pulse length, bandwidth, secondary receivers, beamforming, and tracking which could improve classification performance. We hope to consider many of these concepts in the future.

References

- [1] G.S. Sammelmann and R.H.Hackman, "Acoustic scattering in a homogeneous waveguide", *J. Acoust. Soc. Am.*, Vol. 82, pp. 324-336, 1987.
- [2] N.C. Makris, "A spectral approach to 3-D object scattering in layered media applied to scattering from submerged spheres ", *J. Acoust. Soc. Am.*, Vol.104, pp. 2105-2113, 1998.
- [3] J.A Fawcett, W.L.J. Fox, and A. Maguer, "Modeling of scattering by objects on the seabed ", *J. Acoust. Soc. Am.*, Vol. 104, pp. 3296-3304, 1998.
- [4] P. Chevret, N. Gache, and V. Zimpfer, "Time-frequency filter for target classification", *J. Acoust. Soc. Am.*, Vol. 106, pp. 1829-1837, 1999.
- [5] R.F Dwyer and R.P. Radlinksi, "Sequential classification of active sonar returns", in *proceedings of Oceans '92, Mastering the Oceans through Technology*, Vol. 1, pp. 431-436, 1992.
- [6] G.Okopal, P.J. Loughlin, and L. Cohen, "Dispersion-invariant features for classification", *J. Acoust. Soc. Am.*, Vol. 123, pp.832-841, 2008.
- [7] J. Sildam and J.A. Fawcett, "Baseline classification of acoustical signatures of mine-like objects ", DRDC Atlantic TM 2005-058, 2005
- [8] G. Frisk, *Ocean and seabed acoustics: A theory of wave propagation*, PTR Prentice Hall, 1994.
- [9] F. Ingenito, "Scattering from an object in a stratified medium", *J. Acoust. Soc. Am.*, Vol.82, pp.2851-2859, 1987.
- [10] J.A. Fawcett, "Modelling broadband scattering from shelled spheres in a waveguide", DRDC Atlantic TM 2007-270, 2007.
- [11] A. Tesei, P. Guerrini, and M. Zampolli, "Tank measurements of elastic scattering by a resin-filled spherical shell", in *proceedings of Underwater Acoustic Measurements: Technologies and Results*, F.O.R.T.H., Herkalion, Crete, Greece, 2007.